Supplemental Information for "Symmetry crossover in layered $M\mathbf{PS}_3$ complexes (M = Mn, Fe, Ni) via near-field infrared spectroscopy"

S. N. Neal,[1] H.-S. Kim,[2] K. R. O'Neal,[1] A. V. Haglund,[3] K. A. Smith,[1] D. G. Mandrus,[3] H. A. Bechtel,[4] G. L. Carr,[5] K. Haule,[2] D. Vanderbilt,[2] and J. L. Musfeldt[1,6]

[1]*Department of Chemistry, University of Tennessee, Knoxville, Tennessee 37996, USA*

[2]*Department of Physics and Astronomy, Rutgers University, Piscataway, New Jersey 08854, USA*

[3]*Department of Materials Science and Engineering, University of Tennessee, Knoxville, Tennessee 37996, USA*

[4]*Advanced Light Source Division, Lawrence Berkeley National Laboratory, Berkeley, California 94720, USA*

[5]*National Synchrotron Light Source II, Brookhaven National Laboratory, Upton, New York 11973, USA*

[6]*Department of Physics and Astronomy, University of Tennessee, Knoxville, Tennessee 37996, USA*

(Dated: June 23, 2020)

Far field infrared absorption, Raman scattering, and near field infrared

Figure S1 displays the traditional infrared absorption and Raman scattering response of $MnPS_3$, $FePS_3$, and $NiPS_3$ single crystals at room temperature. This figure also shows (in the bottom set of panels) the corresponding near-field spectra, both amplitude and phase, for each system. The signal-to-noise ratio in the near-field spectrum is much lower than what one achieves with standard far-field infrared techniques. This is because we are dealing with exfoliated flakes that are extremely small in size with little to no optical density. Increasing the number of scans can provide some relief because the signal-to-noise ratio goes as the square root of the number of scans. Additional scans will not, however, make a small spectral feature become larger. On the other hand, this spatially-resolved tip-based nature of the technique is a tremendous advantage when measuring exfoliated sheets.

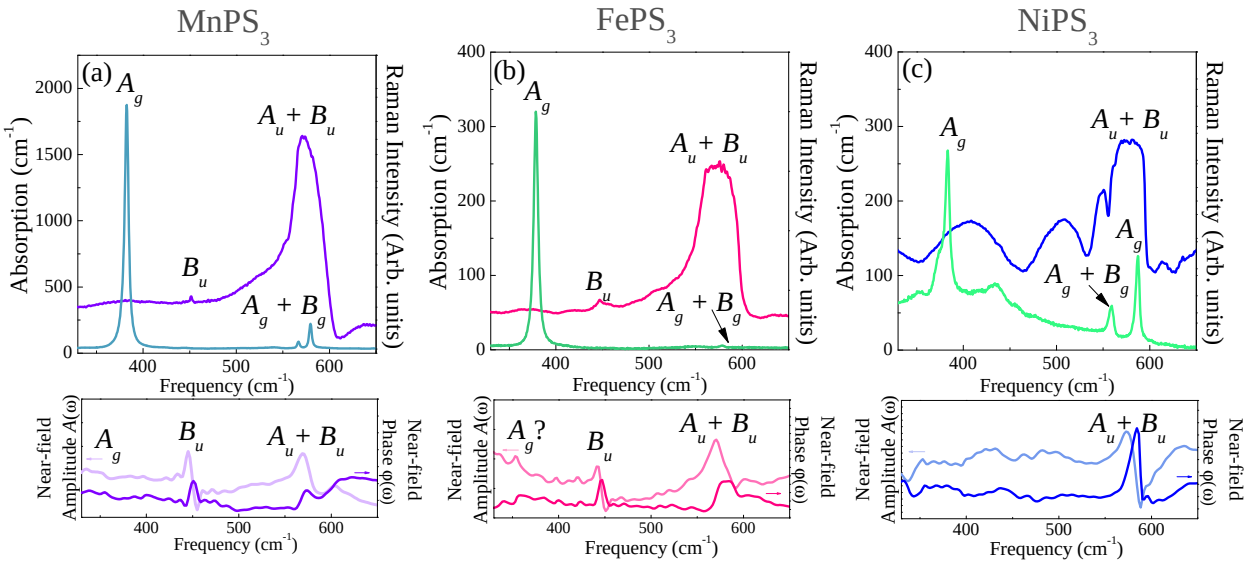

FIG. S1. Top panels (a-c) display traditional infrared absorption and Raman scattering spectra for single crystals of $MnPS_3$, $FePS_3$, and $NiPS_3$ at 300 K. The bottom panels show the near-field infrared amplitude and phase of the corresponding systems.

Vibrational mode assignments

Table S1 summarizes the mode assignments for the MPS_3 (M=Mn, Fe, Ni) family of materials across the currently available near field frequency window (330-700 cm^{-1}). These assignments are made based upon the data in Fig. S1, comparison with literature results, [S1–S4] and our complementary lattice dynamics calculations.

TABLE S1. Vibrational mode assignments of $MnPS_3$, $FePS_3$, and $NiPS_3$ single crystals. All values are in cm^{-1}.[S1–S4]

Material	Infrared	Raman	Near-field*	Assignments
$MnPS_3$	-	385	365	$\nu(PS_3)$
	452	-	450	$T'_{xy}(PS_3) + \nu$(P-P)
	573	567, 581	567, 609	$\nu(PS_3)$
$FePS_3$	-	378	357	$\nu(PS_3)$
	448	-	446	$T'_{xy}(PS_3) + \nu$(P-P)
	572	580	580, 611	$\nu(PS_3)$
$NiPS_3$	-	350, 385	-	$\nu(PS_3)$
	-	435	-	$T'_{xy}(PS_3) + \nu$(P-P)
	548, 575	559, 586	584	$\nu(PS_3)$

ν = symmetric stretch, T' = translational motion, * corresponds to maxima in the phase spectra.

The B_u symmetry vibrational mode is an incisive probe of local symmetry

Figure S2 summarizes the behavior of the B_u symmetry vibrational mode in the MPS$_3$ (M = Mn, Fe, Ni) family of materials. We measured these single crystals in two different ways: using traditional far infrared absorption spectroscopy and via synchrotron-based near field nano-spectroscopy. Both reveal that the Ni compound is special. Figure S2(a) shows that the B_u mode is present in the $MnPS_3$ and $FePS_3$ systems. It is not present in $NiPS_3$. This is consistent with the near-field studies shown in Fig. S2(b) where the B_u symmetry vibrational mode is again missing. These systems have been traditionally assigned to the $C2/m$ space group in their bulk form.[S1, S5, S6] The spectra of $MnPS_3$ and $FePS_3$ are consistent with this assignment. On the other hand, the lack of a B_u vibrational mode in $NiPS_3$ unequivocally demonstrates that the three-fold rotational axis has been restored. This is consistent with $P\bar{3}1m$. Figure S2(c) shows schematically how the presence (or absence) of the B_u vibrational mode is related to the absence (or presence) of the C_3 rotation.

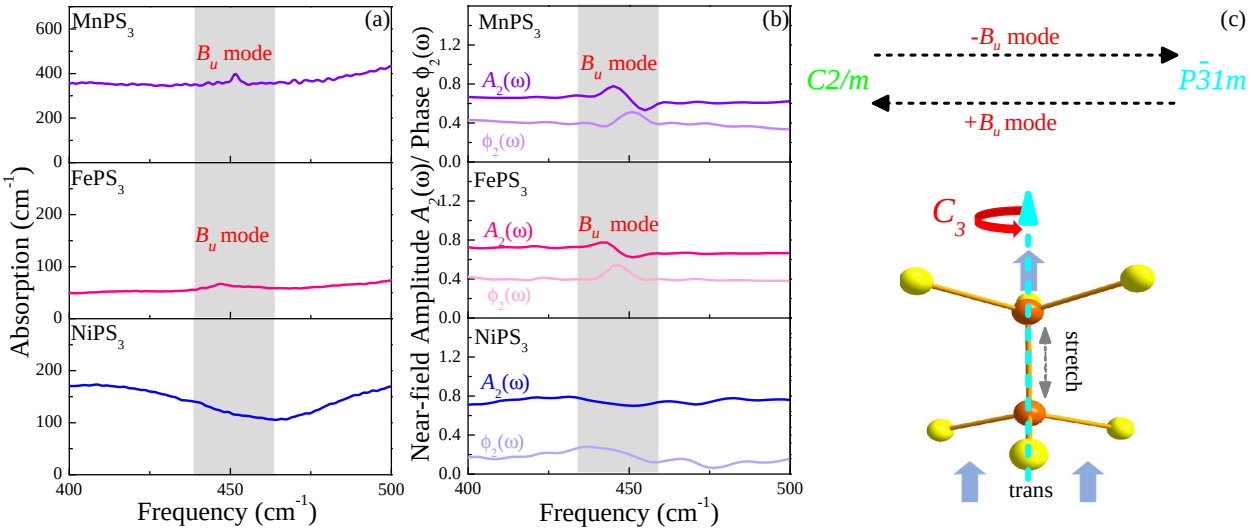

FIG. S2. (a) Close-up view of the B_u vibrational mode in single crystal $MnPS_3$, $FePS_3$, and $NiPS_3$ via traditional far infrared spectroscopy at room temperature. This structure is absent in the Ni compound. (b) Close-up view of the B_u mode in the near field infrared response of the same set of materials. Clearly, the B_u mode is absent in $NiPS_3$ in both far- and near-field studies - even though it is amplified in the near field spectrum of $MnPS_3$ and $FePS_3$. (c) Schematic view of how loss of this particular mode signifies the restoration of a three-fold rotational axis and therefore a symmetry increase to space group to $P\bar{3}1m$. Conversely, the presence of the B_u symmetry feature is microscopic evidence that the system exists in the $C2/m$ space group.

Comparison of local structure in this family of materials

We also summarize the local structure of $MnPS_3$, $FePS_3$, and $NiPS_3$ [Table S2]. [S6, S7] Bond length and angle trends are discussed in the main text along with how these trends dovetail with the crystal symmetry.

Modeling frequency vs. layer number trends

Thinning the crystals to the monolayer is akin to confinement in that the overall length scale is being reduced. To make this more apparent, we fit the layer (thickness) dependent phonon frequencies with a confinement model $\omega = \omega_{bulk}(\frac{q}{r^2})$ in Fig. 3 (c) of the main text. Here, ω is the frequency of the B_u mode of the sheet, ω_{bulk} is the bulk frequency of the same B_u symmetry mode, r is the layer number (which is directly proportional to sheet thickness), and q is a scaling factor that represents the sensitivity of a particular phonon to confinement.

TABLE S2. Bond lengths and angles for the MPS$_3$ (M= Mn, Fe, Ni) family of materials at 300 K.[S6, S7]

Bond/angle type	**MnPS$_3$**	**Number**	**FePS$_3$**	**Number**	**NiPS$_3$**	**Number**
P-S bond (Å)	2.0735	4	2.287	4	1.9905	4
	2.0765	2	2.0323	2	1.9935	2
P-P bond (Å)	2.2154	1	2.2099	1	2.1454	1
M-S bond (Å)	2.5887	3	2.5498	3	2.4993	3
	2.5942	3	2.5567	3	2.4999	3
	2.5818	4	2.5432	4	2.4997	4
S-P-S angle (°)	114.640	2	114.417	2	113.812	2
	114.290	4	114.083	4	113.988	4
S-M-S angle (°)	94.302	2	95.148	2	95.316	2
	94.150	4	94.988	4	94.972	4

Reasonable fits are obtained for each data set by fixing ω_{bulk} as the measured bulk value. This leaves q as the only fitting parameter which is obviously material dependent. We find q = 73 and 53 for MnPS$_3$ and FePS$_3$, respectively. The higher value for MnPS$_3$ indicates that the system is overall stiffer. We find that the fit quality in Fig. 3(c) is better for MnPS$_3$ than for the Fe analog.

[S1] Y. Mathey, R. Clement, C. Sourisseau, and G. Lucazeau. Inorganic Chemistry **19**, 2773 (1980).

[S2] S. N. Neal, H.-S. Kim, K. A. Smith, A. V. Haglund, D. G. Mandrus, H. A. Bechtel, G. L. Carr, K. Haule, D. Vanderbilt, and J. L. Musfeldt. Physical Review B **100**, 075428 (2019).

[S3] P. A. Joy and S. Vasudevan. Journal of Physics and Chemistry of Solids **54**, 343 (1993).

[S4] C. T. Kuo, M. Neumann, K. Balamurugan, H. J. Park, S. Kang, H. W. Shiu, J. H. Kang, B. H. Hong, M. Han, T. W. Noh, and J. G. Park. Scientific Reports **6**, 1 (2016).

[S5] P. A. Joy and S. Vasudevan. Journal of the American Chemical Society **114**, 7792 (1992).

[S6] G. Ouvrard, R. Brec, and J. Rouxel. Materials Research Bulletin **20**, 1181 (1985).

[S7] W. Klingen, E. G., and H. Hanh. Journal of Inorganic and General Chemistry **401**, 97 (1973).